Proceedings of the
International Conference on Mechanical Engineering 2003
(ICME2003) 26- 28 December 2003, Dhaka, Bangladesh

ICME03-KEY-06

ACOUSTICALLY EXCITED AND THERMOACOUSTICALLY INDUCED FLOWS AND HEAT TRANSFER

Bakhtier Farouk and Murat Aktas

Department of Mechanical Engineering and Mechanics
Drexel University
Philadelphia, PA 19104, U. S. A.

ABSTRACT

Convective heat transfer in a differentially heated shallow rectangular enclosure due to the vibration of a vertical side wall is investigated numerically. The frequency of the wall vibration is chosen such that an acoustic standing wave forms in the enclosure. The fully compressible form of the Navier-Stokes equations is considered and an explicit time-marching algorithm is used to explicitly track the acoustic waves. The steady second order flow structures, namely acoustic streaming, are found to be more significant than the primary oscillatory flow field on the cooling rates. The model developed can be used for the analysis of low and temperature fields driven by acoustic transducers. Effects of thermoacoustic wave motion on the developing natural convection process in a compressible gas-filled square enclosure are also investigated numerically. In the cases considered, the left wall temperature is raised rapidly (impulsively or gradually) while the right wall is held at a specified temperature. The strength of the pressure waves associated with the thermoacoustic effect and resulting flow patterns are found to be strongly correlated to the rapidity of the wall heating process.

Keywords: Acoustic streaming, thermoacoustic waves.

1. INTRODUCTION

Effects of oscillatory flow fields on heat transfer can be found in various industrial applications. A detailed understanding of the transport phenomena in these problems is challenging. Sound sources whose parts move essentially sinusoidally may generate a field in which the particle velocities are not simply sinusoidal and a pattern of steady vortices is often found in the body of the irradiated fluid. Sound at high intensity levels in gases and liquids is accompanied by these second order steady flow patterns known as 'acoustic streaming'.

In the containerless processing of materials under reduced gravity conditions [1] alloy samples are acoustically levitated to avoid physical contact with the container walls. Acoustic levitation involves the creation of sufficiently strong and suitably shaped acoustic fields. However, the required high intensity level sound fields give rise to strong acoustic streaming flows around samples and on the walls of the test cells. Acoustic streaming also allows forced convective heat transfer without any macroscopic mechanical moving part by standing wave formation in compressible mediums. With suitable design, this steady vortex flow can be employed for cooling of electronic systems in micro-gravity environment where free convective flows in fluids are greatly reduced or completely eliminated.

Several research studies were conducted in order to achieve a better understanding of the physical mechanism of interaction between free convection and sound. Kawahashi et al. [2] studied the coupling of natural convective with acoustic streaming flows in a horizontal duct heated from below both experimentally and numerically.. Mozurkewich [2] investigated the heat transfer from a cylinder in an acoustic standing wave, experimentally. A paper by Gopinath and Harder [3] described the results of an experimental study on the convective heat transfer behavior from a cylinder in an intense acoustic field. The results of an experimental study on heat transport within a cylindrical resonance tube, mediated by acoustic streaming were reported by Mozurkewich [4].

When a compressible fluid is subjected to a rapid temperature increase at a solid wall, part of the fluid in the immediate vicinity of the boundary expands. This gives rise to a fast increase in the local pressure, and leads to the production of pressure waves called thermoacoustic waves. The heat transfer effects of such waves may be very significant when the fluid is close to the thermodynamic critical point or when other modes of convection are weak or absent. This motion may cause unwanted disturbances in otherwise static processes like cryogenic storage or may introduce a convective heat transfer mode to the systems in zero-gravity environment where it is assumed that conduction is the only heat transfer mode. Low-heat-diffusivity character of near-critical-conditions makes thermoacoustic

convection mode of heat transport very significant for cryogenic storage systems which involve rather weak diffusive and convective transport of heat especially in reduced gravity environment. Because of high density and compressibility values of fluids in these systems, strong thermoacoustic waves are produced and heat transfer effects of these waves become critical due to the possibility of sudden phase change in the storage system. The problem of thermoacoustic waves in a quiescent semi-infinite body of a perfect gas, subjected to a step change in temperature at the solid wall was studied analytically[5] in order to determine how the sound intensity depends on the wall temperature history. The one-dimensional compressible flow equations were linearized and a closed-form asymptotic solution was obtained using a Laplace transform technique. A simplified model (the hyperbolic equation of conduction) for thermoacoustic motion was compared with one-dimensional Navier-Stokes equations model of the phenomena and limitations of the simplified approach was discussed [6]. A more general class of solutions for the thermoacoustic waves was obtained by using the Laplace transform method with numerical inversion for equations of the linear wave model for step and gradual changes in the boundary temperature [7]. The equations of the nonlinear wave model were numerically solved using finite differences scheme modified with a Galerkin finite element interpolation in space. A similar analysis for thermoacoustic waves in a confined medium was repeated more recently

In the present study, we investigate the heat transfer in a rectangular enclosure (Fig. 1) due to primary oscillatory and secondary steady flow fields, numerically. The oscillatory flow field in the nitrogen-filledenclosure is created by the vibration of the left wall of the enclosure. Initially the gas is quiescent and at T0 = 300K. The frequency of the wall vibration is chosen such that an acoustic standing wave forms in the enclosure (f = 20 kHz). Corresponding wavelength of the sound waves at this frequency is l = 17.65 mm based on the sonic speed in nitrogen (c = 353 m/s). The interaction of this wave field with the solid boundary and resulting acoustic boundary layer formation leads to the production of inner and outer acoustic streaming flow patterns in the enclosure. The length and the height of the enclosure are L = 8.825 mm and H = 0.316 mm, respectively. The length of the enclosure corresponds to a half wavelength and the ratio of the height of the enclosure to the acousticboundary layer thickness (δac) is twenty.

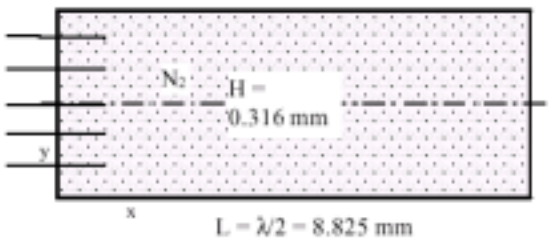

Figure 1. Schematic of the problem.

The effects of thermoacoustic waves on buoyancy-induced flow fields are also studied for a square enclosure with side length L = 13 mm. The horizontal walls of the square enclosure are considered to be insulated whereas the vertical walls are isothermal. Initially the gas and all walls are in thermal equilibrium. The left wall temperature is increased either suddenly or gradually. The strength of the thermoacoustic waves depend on the rapidity of the wall heating, and the interaction effects are significant only for the early times. We also investigate the effects of fluid properties on the interaction process.

2. MATHEMATICAL MODEL

Effect of oscillatory flow fields and acoustic streaming structures on heat transfer in a two-dimensional enclosure is described by the Navier-Stokes equations for a compressible fluid. These equations are expressed as:

$$\frac{\partial \rho}{\partial t}+\frac{\partial(\rho u)}{\partial x}+\frac{\partial(\rho v)}{\partial y}=0 \tag{1}$$

$$\rho\frac{\partial u}{\partial t}+\rho u\frac{\partial u}{\partial x}+\rho v\frac{\partial u}{\partial y}=-\frac{\partial p}{\partial x}+\frac{\partial \tau_{xx}}{\partial x}+\frac{\partial \tau_{xy}}{\partial y} \tag{2}$$

$$\rho\frac{\partial v}{\partial t}+\rho u\frac{\partial v}{\partial x}+\rho v\frac{\partial v}{\partial y}=-\frac{\partial p}{\partial y}+\frac{\partial \tau_{yy}}{\partial y}+\frac{\partial \tau_{xy}}{\partial x}+\rho g \tag{3}$$

$$\frac{\partial E}{\partial t}+\frac{\partial}{\partial x}\left[(E+p)u\right]+\frac{\partial}{\partial y}\left[(E+p)v\right]=\frac{\partial}{\partial x}\left[u\tau_{xx}+v\tau_{xy}\right]+\frac{\partial}{\partial y}\left[u\tau_{xy}+v\tau_{yy}\right]-\frac{\partial q_x}{\partial x}-\frac{\partial q_y}{\partial y}+\rho v g \tag{4}$$

Here t is time, x and y refer to the Cartesian coordinates, r is density, p is pressure, u and v are the velocity components and E is the total energy given by;

$$E=\rho c_v T+\frac{1}{2}\rho(u^2+v^2) \tag{5}$$

The components of the stress tensor τ are;

$$\tau_{xx}=\frac{4}{3}\mu\frac{\partial u}{\partial x}-\frac{2}{3}\mu\frac{\partial v}{\partial y} \qquad \tau_{yy}=\frac{4}{3}\mu\frac{\partial v}{\partial y}-\frac{2}{3}\mu\frac{\partial u}{\partial x}$$

$$\tau_{xy}=\mu\left(\frac{\partial u}{\partial y}+\frac{\partial v}{\partial x}\right) \tag{6}$$

where μ is the dynamic viscosity. The components of the heat-flux vector are written as;

$$q_x=-k\frac{\partial T}{\partial x} \qquad q_y=-k\frac{\partial T}{\partial y} \tag{7}$$

where k is thermal conductivity and T is temperature. The temperature is related to the density and pressure through the ideal-gas law:

$$p=\rho RT \tag{8}$$

where R is the specific gas constant of the medium.

3. NUMERICAL SCHEME

The governing equations (except for the diffusion terms) are discretized using a control-volume-based flux-corrected transport (FCT) algorithm. FCT is a high order, nonlinear, monotone, conservative and positivity-preserving scheme designed to solve a general

one-dimensional continuity equation with appropriate source terms. This scheme has fourth-order phase accuracy and is able to resolve steep gradients with minimum numerical diffusion. In this algorithm, when a flow variable such as a density is initially positive, it remains positive during the computations and no new minimum or maximum values are introduced due to numerical errors in the calculation process. To ensure positivity and stability, a minimum amount of numerical diffusion over the stability limit is added at each time step. Time-step splitting technique is used to solve the two-dimensional problem addressed here. Further details of the FCT algorithm used here are documented by Boris et al. [8]. The diffusion terms in the momentum equations and the conduction terms in the energy equation are discretized using the central-difference approach and the time-step splitting technique is used to include the terms in the numerical scheme.

No-slip boundary conditions are used for all solid walls. A high-order non-dissipative algorithm such as FCT requires rigorous formulation of the boundary conditions. Otherwise, numerical solutions may show spurious wave reflections at the regions close to boundaries and nonphysical oscillations arising from instabilities. In the present computational method, the treatment proposed by Poinsot and Lele [9] is followed for implementing the boundary conditions for the density. This method avoids incorrect extrapolations and overspecified boundary conditions. Along any stationary solid wall, the density is calculated from;

$$\left(\frac{\partial \rho}{\partial t}\right)_M + \frac{1}{c_M}\left(\frac{\partial p}{\partial n} + \rho c \frac{\partial u_n}{\partial n}\right)_M = 0 \qquad (9)$$

where c_M is the acoustic speed, M indicates the location of the wall and n is the direction normal to the wall. Since the current problem involves a moving boundary and a time dependent boundary velocity, a modification in this part of the scheme is required for the left boundary. Along the vibrating wall, the density is calculated from;

$$\frac{\partial \rho}{\partial t} = \frac{\rho\gamma}{c_L}\frac{\partial u_W}{\partial t} + \frac{\rho\gamma(u_W - c_L)}{c_L}\frac{\partial u}{\partial x} - \frac{\gamma(u_W - c_L)}{c_L^2}\frac{\partial p}{\partial x} \qquad (10)$$

where c_L is the acoustic speed at the left wall.

Acoustic streaming flows in high-intensity sound fields are characterized by two different types of circulatory steady flow structures. The circulations forming in the immediate vicinity of the viscous boundaries are referred as ‘inner’ or Schlichting type of acoustic streaming. The inner streaming structures give rice to the second type of streaming called ‘outer’ or Rayleigh streaming observed outside of the viscous layers. Inner and outer streaming motions have opposite rotation.

Since the formation of acoustic streaming structures results from the interaction between the wave field andthe viscous boundary, resolving the acoustic boundary layer, $\delta_{ac} = \sqrt{2\nu/\omega}$, in the computational method is a required condition to accurately predict the inner acoustic streaming structures. For this reason, we employ a non-uniform grid structure with 121´111 computational cells for these simulations. This grid structure has very fine grids in the vicinity of the top and bottom walls of the enclosure and the grid quality gradually decreases with the increasing vertical distance from the walls. In this grid structure, the variation of the left wall position and the size changes for the first column cells were also taken into account since the problem involves the modeling of a vibrating wall.

4. RESULTS AND DISCUSSION

Acoustically Excited Flows

We performed the simulations for three cases in this study. For each case, the calculations were started with the vibration of the left wall at x = 0 and with uniform values of pressure, temperature and density within a quiescent medium. For each cycle of the vibrating wall, about 25,000 time steps were used for the computations. All results are for zero-gravity conditions.

In the first case considered (CASE- 1), the heating is applied on the vibrating left wall of the enclosure (T_L = 310 K) and the right wall of the enclosure is kept at ambient temperature $T_R = T_0$ = 300 K. The top and the bottom walls of the enclosure are thermally insulated. The displacement of the vibrating wall is given by $s = s_m \sin(wt)$. Here, s_m is the maximum displacement of the wall, ω is the angular frequency of the vibration ($\omega = 2\pi f$) and $s_m\omega$ product represents the maximum velocity of the wall. The maximum displacement of the wall is set to s_m= 10 μm.

Fig. 2 shows the pressure distribution along the horizontal mid-plane of the enclosure at wt = 0, π/2, π, 3π/2 (during cycle # 101).

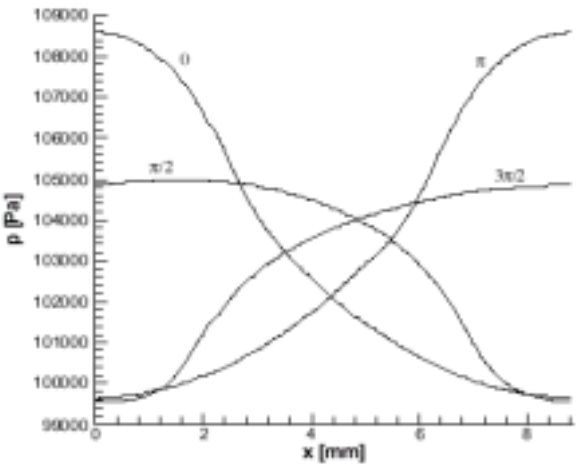

Figure2. Variation of pressure along the horizontal mid-plane of the enclosure at four different instant (ωt=0,π/2,π,3π/2) during the acoustic cycle starting at t=5 ms (CASE-1).

These pressure profiles remain the same at any other horizontal plane far from the bottom and top walls and this indicates the near-one-dimensional character of the acoustic field. The pressure distribution for $\omega t = 2\pi$ (not shown here) is identical to the curve given for ωt = 0. At ωt = 0 and $\omega t = \pi$, the amplitude of the pressure waves reach a maximum value in the enclosure. At the beginning of the cycle (ωt = 0), the pressure is maximum on the vibrating (left) wall of the enclosure and

decreasing with increasing distance from the wall and reaching a minimum at $x \cong L/2$. In second half of the enclosure ($L/2 < x < L$), the pressure profile shows fairly symmetric behavior to the first half and reaches a maximum at the right wall. The pressure profiles given for different time levels forms the pressure nodes at approximately $x = L/2$. It is noted here that thermoacoustic waves (induced by sudden heating of the left wall) [13; 14] damped out at 5 ms (Fig. 2).

Corresponding u-velocity profile for this case is given in Fig. 3. Unlike the pressure field, velocity maximums and minimums are observed at $\omega t = \pi/2$ and $\omega t = 3\pi/2$. The left wall is stationary at $\omega t = \pi/2$ and $wt = 3\pi/2$. The oscillatory flow is periodic and the maximum velocity value is predicted approximately 11 m/s in this primary flow field.

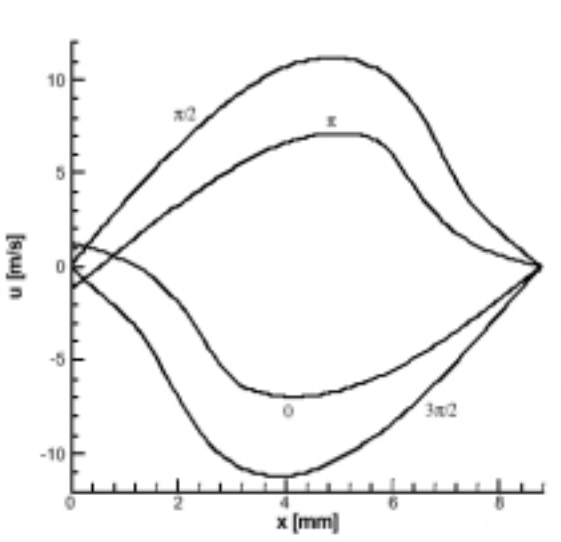

Figure 3. Variation of u velocity along the horizontal mid-plane of the enclosure at four different instant ($\omega t=0,\pi/2,\pi,3\pi/2$) during the acoustic cycle starting at t= 5 ms (CASE-1)

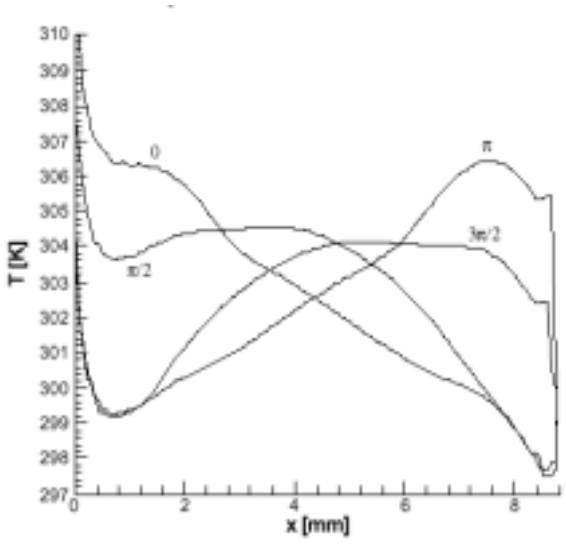

Figure 4. Variation of temperature along the horizontal mid-plane of the enclosure at four different instants ($\omega t=0,\pi/2,\pi,3\pi/2$) during the acoustic cycle starting at t= 5 ms(CASE-1)

Fig. 4 shows the instantaneous temperature profiles during the same acoustic cycle in the enclosure. Far from the heated (left) wall, temperature profiles are also periodic in nature. However, the temperature field is characterized by the diffusion dominated transport close to left wall.

The predicted secondary flow field is shown in Fig 5. This flow field is based on the time averaged velocity values in the enclosure. For the results shown in Figure 5, the time averaging was applied during the 100 th vibration cycle of the left wall and gives the streaming velocity values at t = 5 ms. The time-averaged velocities have become cycle-independent by this time. The maximum steady streaming velocity value is at the order of 0.06 m/s, although the instantaneous velocities reach 11 m/s in the primary flow field for this case. Four different circulations in clock wise and counter clock wise directions are observed. The size of the circulatory flow structures (inner streaming) observed in the vicinity of the horizontal walls is characterized by the thickness of the acoustic boundary layer. The streaming structures seen in the middle section of the enclosure (outer streaming) have larger size. Predicted streaming structures and velocity values are in good agreement with the results presented by Hamilton et al. [15] in a recent study.

Figure 5. Flow field in the enclosure based on the time averaged velocities at t = 5 ms (CASE-1). Fig. 6 shows the time averaged temperature profile along the horizontal plane for CASE-1. For comparison, an enclosure having identical geometry and temperature boundary conditions but without any acoustic excitation (stationary left wall) is also considered and the predicted temperature profile for this problem is also included in the same figure. There is no wave formation and periodic fluid motion in the enclosure for this configuration. Although very weak fluid motion (at the order of 0.001 m/s) due to compressible nature of the fluid is observed (not shown here) in the enclosure for this case, thermal diffusion dominates the heat transport in the system. A sharp temperature gradient is observed at the left wall and a local temperature peak appears in the center region of the geometry due to weak fluid motion (velocity node). Time variation of the average heat transfer coefficient for the left wall during the first 100 cycle is given in Fig. 7 for the CASE-1. Initially heat transfer is high due to the large temperature difference between the wall and the gas. After approximately 10 cycles, the variation of the heat transfer coefficient is characterized by the oscillatory fluid motion in the enclosure. The heat transfer coefficient is defined as;

$$h = \frac{-k\dfrac{\partial T}{\partial x}}{\left|T_L - T_R\right|} \qquad (11)$$

Time (cycle) averaged value of the left wall heat transfer coefficient is given in Fig. 8. The predicted values of heat transfer coefficient for the case without

vibrating boundary are also included in the figure. The figure indicates that the overall heat transfer with streaming

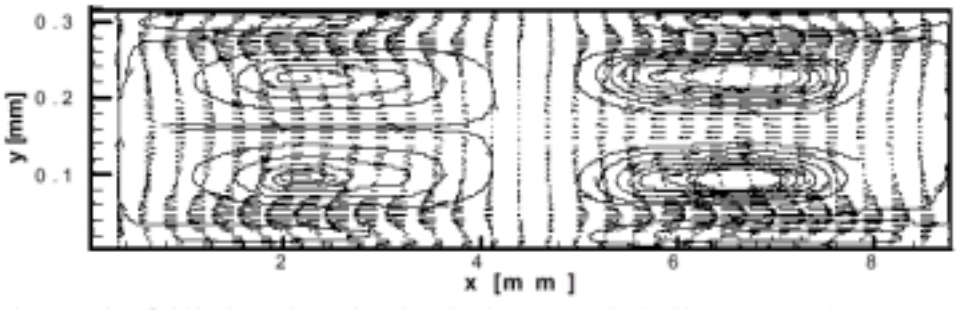

Figure 5. Flow fiels in the enclosure based on the time averaged velocities at t= 5 ms (CASE 1)

motion is higher compared to the case without oscillatory fluid motion. The left wall heat transfer coefficient reached to a quasi-steady value of 0.2 W/m 2 K.

To further investigate the physical reason of the observed heat transfer increasein enclosures with oscillatory flows we consider a case (CASE-2) with a different left wall vibration frequency (from 20 kHz to 25 kHz). A comparison with the similar time averaged flow field given for CASE-1 (Fig. 5) clearly indicates that the regular clock wise and counter clock wise circulating acoustic streaming structures are not observed for the increased value of the vibration frequency.

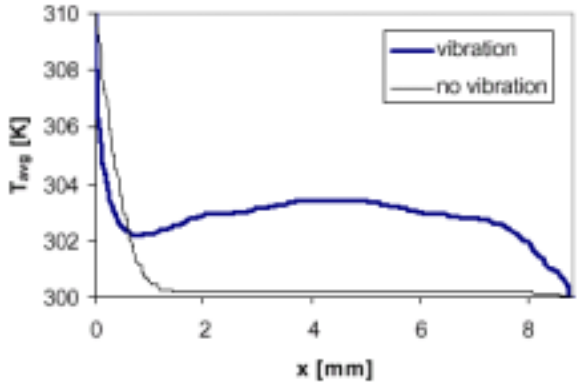

Figure 6. Time averaged temperature profile along the horizontal mid-plane of the enclosure at t=5 ms (CASE-1_.

Fig. 9 shows the time variation of the instantaneous values of the left wall heat transfer coefficient. The effect of the primary oscillatory flow field is evident on the heat transfer characteristics of the enclosure. However, thetime (cycle) averaged values of the heat transfer coefficient for the system with 25 kHz vibration frequency is not very different than from those given for the enclosure with a stationary left wall. No significant augmentation in the overall heat transfer rate obtained with the addition of the vibrating boundary and the resulting oscillatory flow. This result demonstrates the significant effect of the steady second order streaming motion in the heat transfer characteristics of the systems. Streaming structures introduce an additional circulatory motion that greatly contributes to the convective heat transfer in the system. Oscillatory primary flow fields (x-directional) cannot provide the efficient cooling without streaming structures although the primary flow velocities are two orders of magnitude larger than the steady streaming velocities.

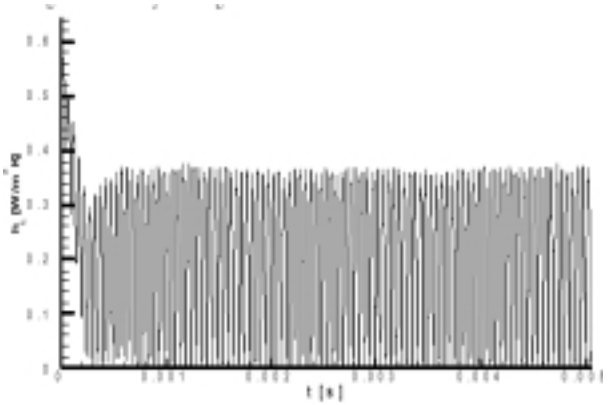

Figure7. Temporal variation of the left wall heat transfer coefficient (CASE-1)

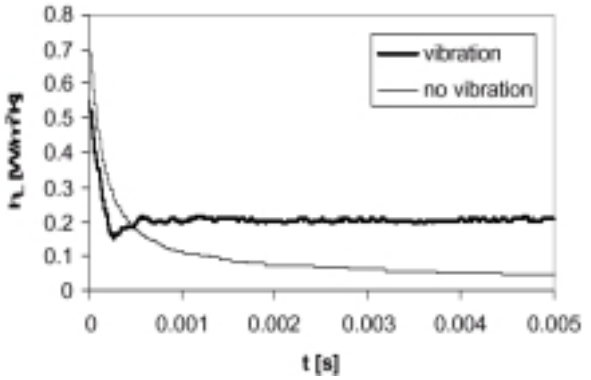

Figure 8. Temporal variation of the time averaged left wall heat transfer coefficient (CASE-1)

In the next case considered (CASE-3), the heating is applied on the stationary right wall of the enclosure (T_R= 310 K). The vibration amplitude of the left wall is kept at the same value with the CASE-1 and the temperature of the left wall is kept at ambient temperature $T_0 = T_L = 300$

K. The predicted pressure amplitudes and primary flow field velocities for this case are fairly close (not shown here) to those given for CASE-1. The wave field determined by the vibrating boundary and the heating condition has negligible effect on the secondary flow structures (not shown here).

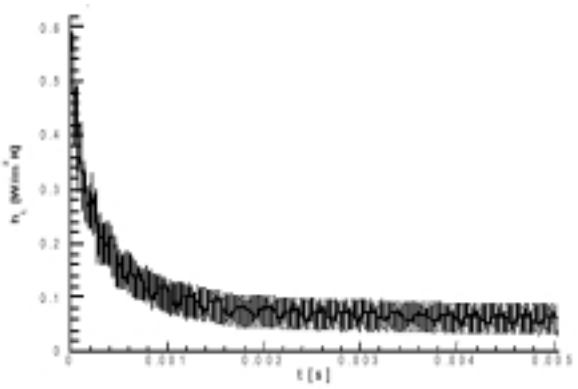

Figure 9. Temporal variation of the left wall heat transfer coefficient (CASE-2).

Fig. 10 shows the time averaged temperature profile along the horizontal plane of the enclosure for CASE-3.Same figure also includes the predicted temperature profile for an enclosure without vibrating wall. The profiles are fairly symmetric to the results given for the enclosure heated from left wall.

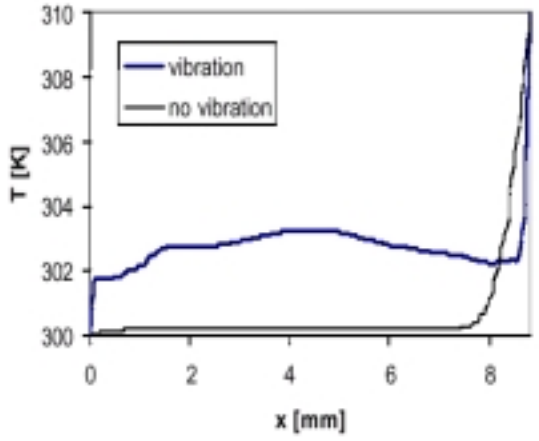

Figure 10. Time averaged temperature profile along the horizontal mid-plane of the enclosure at t=4 ms (CASE-3)

The figure indicates that the overall heat transfer with streaming motion is higher compared to the case without oscillatory fluid motion. The right wall heat transfer coefficient reached to a quasi-steady value of 0.17 W/m 2 K. This value is slightly smaller than the coefficient computed for CASE-1 in which the vibrating left wall is also the heated wall.

Thermoacoutically driven flows

Numerical simulations of the thermoacoustic wave motion and its interactions with the buoyancy-induced flow fields were performed for a square enclosure filled with nitrogen gas, initially quiescent at 1 atm pressure and 300 K temperature. For all computations, non-uniform grid structure was employed with 141´141 computational cells. Variation of the fluid properties with temperature was taken into account. Results of our prior investigation [10] on the very short time behavior of the thermoacoustic waves generated by impulsive and gradual heating of a wall were in very good agreement with the results given in the literature. In the present study, longer time behavior of the pressure waves produced by a step change (impulsive heating) at the left wall temperature of the enclosurewas investigated. For impulsive heating, the left wall temperature is given by

$$T_L^* = \begin{cases} T_0^* & ;t^* = 0 \\ T_0^*(A+1) & ;t^* > 0 \end{cases}$$

Where T_o is the initial temperature ($T^*_0=T^*_R$) and A is the overheat ratio.

$$A = \frac{T_L^* - T_R^*}{T_R^*} \qquad (12)$$

In a numerical scheme, 'impulsive heating' can be approximated by the value of the first time step. In the present computations the first time step is rather small, $1.04\text{x}10^{-7}$ s. In practice, due to the thermal inertia of a wall and a heating system and unavoidable heat losses to the environment, it is difficult to generate a step change (impulsive heating) in the wall temperature.

Figs. 11a - 11d show the velocity vectors for the case where A = 1/3 and Ra = 10^4 . All four figures show the velocity field in the enclosure at a given time (t * = 0.025 s; t = $4.2675\text{´}10^{-3}$), with different heating conditions of the left wall. For impulsive heating, (Fig. 11a), very strong back flow is observed as a result of the pressure wave reflection on the right wall. This behavior significantly changes in case of gradual heating ($\tau_h = \tau_c$, Fig. 11b; $\tau_h = 5\tau_c$, Fig. 11c; $\tau_h = 20\tau_c$, Fig. 11d). It is interesting to note that though the characteristic time for acoustic wave propagation in the enclosure (τ_c = $36.82\text{x}10^{-6}$ s) is rather small, the effects of the thermoacoustic waves are significant even at t * = 0.025 s, as shown in Fig. 11a for impulsive heating.

Traditional computational fluid dynamics techniques employing pressure-velocity formulation of the Navier-Stokes equations fail to predict the thermoacoustic effect on the transient buoyancy driven motion for rapid heating. In earlier studies [11, 12], the signature of the thermoacoustic waves were not reported accurately–perhaps due to significant numerical diffusion and the lack of 'characteristic (wave)' type wall boundary conditions in the scheme [9]. The flow fields given in the earlier papers also do not clearly demonstrate the effects of thermoacoustic waves on the buoyancy-induced flows.

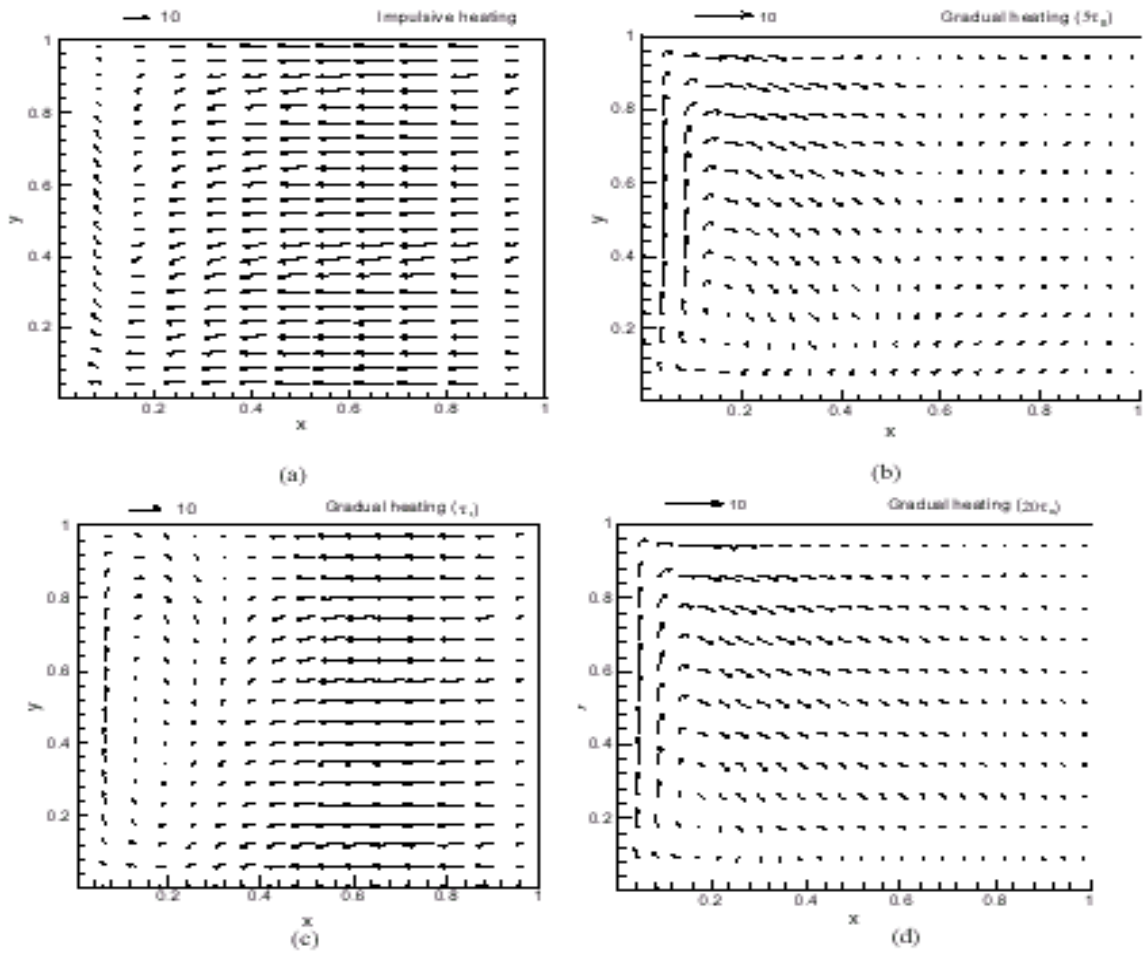

Figure 11. Variation of the velocity vectors and flow field depending on the rapidity of the wall heating process at $Ra=10^4$,t= $4.2675x10^{-3}$ (t*=0.025 s.) a)Impulsive heating, b)Gradual heating (τ_c) c) Gradual heating ($5\tau_c$) d) Gradual heating ($20\ \tau_c$).

5.DISCUSSION

The effects of the oscillatory primary flow field and the resulting steady second order acoustic streaming structures on developing heat convection process in a nitrogen-filled shallow enclosure were studied computationally. The mechanically induced periodic oscillations in the fluid are found to be insignificant on the heat transfer characteristics of the system, unless steady streaming flows are present also. Cooling rates in the enclosure are significantly enhanced by the second order steady acoustic streaming flow structures. Acoustic streaming introduces an additional convective heat transfer mode in to the systems in zero-gravity environment where it is assumed that conduction is the only heat transfer mode. The effects of the thermoacoustic phenomena on the transient natural convection process in an enclosure were studied by solving the unsteady compressible Navier-Stokes equations. The effects of the pressure (thermoacoustic) waves on the transient natural heat convection process and flow development were also determined. Thermoacoustic waves were generated by increasing the left wall temperature of the enclosure impulsively (suddenly) or gradually and rapidity of the wall heating process was observed to be the leading parameter on the strength of the thermoacoustic waves.

6. REFERENCES

1. Gopinath, A., and Mills, A. F. 1993. "Convective heat transfer from a sphere due to acoustic streaming".Journal of Heat Transfer 11**5:** 332.

2. Mozurkewich, G. 1995. "Heat transfer from a cylinder in an acoustic standing wave". Journal of the Acoustical Society of America 9**8:** 2209.

3. Gopinath, A., and Harder, D. R. 2000. "An experimental study of heat transfer from a cylinder in low-amplitude zero-mean oscillatory flows". International Journal of Heat and Mass Transfer 4**3:** 505.

4. Mozurkewich, G. 2002. "Heat transport by acoustic streaming within a cyclindrical resonator". Applied Acoustics 6**3:** 713.

5. Trilling, L. 1955. "On thermally induced sound fields". Journal of the Acoustical Society of America 2**7** 425.

6. Churchill, S. W., and Brown, M. A. 1987. "Thermoacoustic convection and the hyperbolic equation of conduction". International Communications in Heat and Mass Transfer 1**4:** 647.

7. Huang, Y., and Bau, H. H. 1995. "Thermoacoustic waves in a semi-infinite medium". International Journal of Heat and Mass Transfer 3**8:** 1329.
8. Boris, J. P., Landsberg, A. M., Oran, E. S., and Gardner, J. H. 1993. LCPFCT- A flux-corrected transport algorithm for solving generalized continuity equations, Naval Research Laboratory, Washington, DC.
9. Poinsot, T. J., and Lele, S. K. 1992. "Boundary conditions for direct simulations of compressible viscous flows". Journal of Computational Physics 10**1:** 104.
10. Farouk, B., Oran, E. S., and Fusegi, T. 2000. "Numerical study of thermoacoustic waves in an enclosure". Physics of Fluids 1**2:** 1052.
11. Ozoe, H., Sato, N., and Churchill, S. W. 1980. "The effect of various parameters on thermoacoustic convection". Chemical Engineering Communications **5:** 203.
12. Ozoe, H., Sato, N., and Churchill, S. W. 1990. "Numerical analyses of two and three dimensional thermoacoustic convection generated by a transient step in the temperature of one wall". Numerical Heat Transfer, Part A 1**8:** 1.

7. NOMENCLATURE

Symbol	Meaning
E	total energy
g	gravitational acceleration
h	heat transfer coefficient
k	thermal conductivity
L	width of the enclosure
P	pressure
q	heat flux
R	specific gas constant
t	time
T	temperature
u	velocity in the horizontal direction
v	velocity in the vertical direction
x	horizontal direction
y	vertical direction
Greek symbols	
α	thermal diffusivity
β	volumetric thermal expansion coefficient, (= 1/Tf *)
γ	ratio of specific heats
μ	dynamic viscosity
ν	kinematic viscosity
ρ	density
τ	shear stress
t_c	travel time for the acoustic wave to traverse the enclosure width
t_h	time constant for wall heating
Subscripts	
0	initial
L	left
M	wall location
n	direction normal to the wall
R	right